JOURNAL OF MATERIALS SCIENCE 24 (1989) 2541–2548

A study of Nd–Fe–B magnets produced using a combination of hydrogen decrepitation and jet milling

P. J. McGUINESS, E. DEVLIN, I. R. HARRIS
Department of Metallurgy and Materials, University of Birmingham, Edgbaston, B15 2TT, UK
E. ROZENDAAL, J. ORMEROD
Mullard Southport, Merseyside PR9 8PZ, UK

A combination of hydrogen decrepitation (HD) and jet milling (JM) has been used to produce powder for the processing of permanent magnets. The procedure has proved to be very successful for both Nd–Fe–B (Neomax) alloys and the Nd–Dy–Fe–Nb–B high coercivity alloys. The magnets produced by the HD/JM process showed excellent coercivities when sintered between 980 and 1040° C; at higher temperatures, excessive grain growth reduced the coercivity values significantly.

1. Introduction

The use of hydrogen in the processing of rare-earth magnets has been studied in the Department of Metallurgy and Materials, University of Birmingham, since 1978. These experiments have been reviewed [1, 2]. Early work [1–3] concerned hydrogen decrepitation (HD) of the intermetallic $SmCo_5$ and sintered and polymer-bonded magnets were produced from hydrogen-decrepitated powder. In the case of $SmCo_5$, hydrogen could be absorbed and desorbed at room temperature prior to the magnetic alignment and compaction procedure.

The HD process was extended to $Sm_2(Co, Fe, Cu, Zr)_{17}$-type magnets [4, 5] and for these materials the combination of high hydrogen pressure and a temperature of 200° C was required to complete the process. Sintered magnets were produced by aligning the hydrided powder and the hydrogen was subsequently removed during the vacuum sintering operation [6].

Soon after the announcement of the Nd–Fe–B Neomax magnetic alloy [7] we reported on the effect of exposing the alloy to hydrogen at room temperature [8]. These studies showed that the material reacted readily with hydrogen at moderate pressures with a strongly exothermic reaction. Work on the desorption of hydrogen from the $Nd_{16}Fe_{76}B_8$ alloy [8] indicated that vacuum degassing consisted of two stages whereby hydrogen was first desorbed from the $Nd_2Fe_{14}B$ matrix phase below 300° C, with the remainder being evolved from the neodymium-rich phase between 350 and 650° C.

The formation of two hydrides is consistent with the decrepitation behaviour where the initial activation process corresponds with the hydriding of the intergranular, neodymium-rich material, followed by the

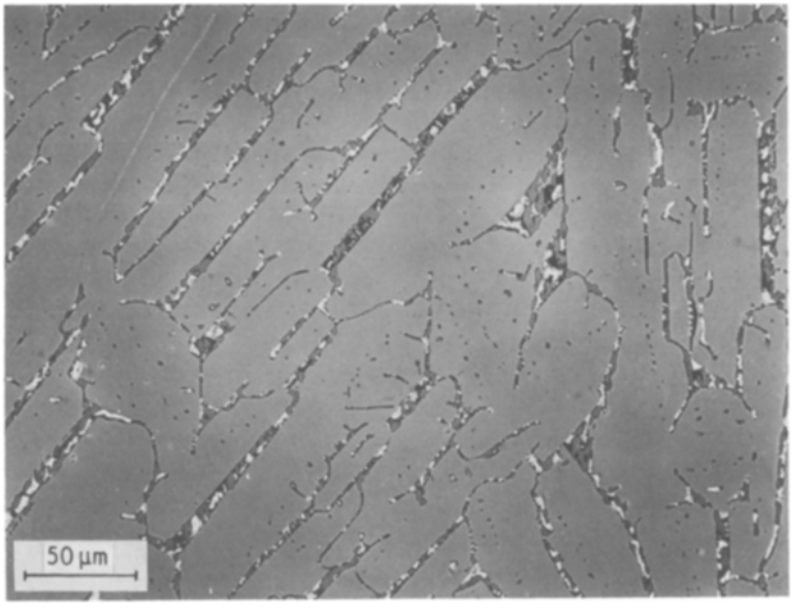

Figure 1 A general view of the microstructure of an as-cast ingot of the alloy $Nd_{16}Fe_{76}B_8$.

0022–2461/89 $03.00 + .12

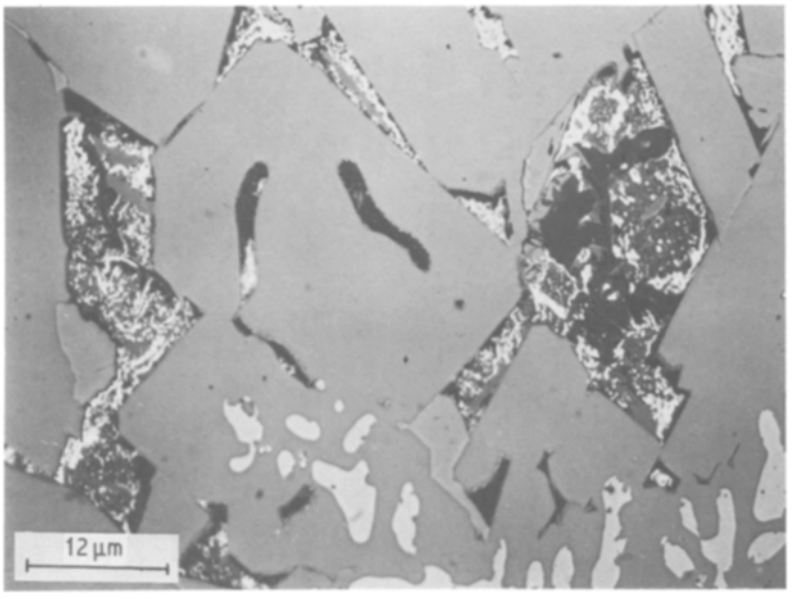

Figure 2 Details of the microstructure of an as-cast ingot of the alloy $Nd_{16}F_{76}B_8$. The arrow indicates the presence of some free iron.

hydriding of the matrix phase with the attendant transcrystalline cracking of the individual crystallites.

Work on the production of a Nd–Fe–B magnet using hydrogen decrepitation as a method of pre-milling the powder was initiated by Harris *et al.* [8], and a comprehensive study has been carried out in conjunction with Mullard Southport and Lucas Research Centre [9]. A bulk ingot of a Nd–Fe–B alloy was powdered by a combination of hydrogen decrepitation and attritor milling (HD/AM). The powder was aligned and pressed in the hydrided condition and the green compact sintered at 1080° C for 1 h. The magnets produced using this process showed good sintered densities and energy products of around 250 kJ m^{-3}. In a recent paper [10] the hydrogen absorption/desorption behaviours of the alloy $Nd_{16}Fe_{76}B_8$ and $Nd_2Fe_{14}B$ have been examined. These studies reveal clearly the essential role of the neodymium-rich grain boundaries in the $Nd_{16}Fe_{76}B_8$ alloy in the hydrogen activation process.

Reports of other groups carrying out similar studies are scarce. Cadogan and Coey [11] have produced results on the hydrogen absorption and desorption properties of $Nd_{15}Fe_{77}B_8$ alloys but magnets were not produced from the resulting powders. Pollard and Osterreicher [12] have also reported on the hydriding of Neomax-type alloys, and have proposed a route for producing fine powder direct from the hydrogen decrepitation process. However, no results of the production of permanent magnets from this powder have been published. Fruchart *et al.* [13] have also reported on the use of hydrogen to produce powder of the stoichiometric $Nd_2Fe_{14}B$ phase. This patent however did not give any information on the production of magnets.

In our previous paper [9] on the HD/AM process we were of the opinion that "the HD process would be more effective if combined with jet milling". Thus in this paper we report on the application of the hydrogen decrepitation process in conjunction with jet milling (HD/JM), to the production of Nd–Fe–B magnets from bulk alloys with composition $Nd_{16}Fe_{76}B_8$ and $Nd_{14.5}Dy_{1.5}Fe_{76}NbB_7$.

2. Experimental procedure

2.1. Material

The bulk alloys were prepared by induction-melting the constituents and the microstructure of the alloys were investigated by polishing sections and examining in an optical microscope. For example, the as-cast microstructure of the $Nd_{16}Fe_{76}B_8$ alloy is shown in Figs 1 and 2, the former showing the typical columnar grain structure and the latter showing the details of the

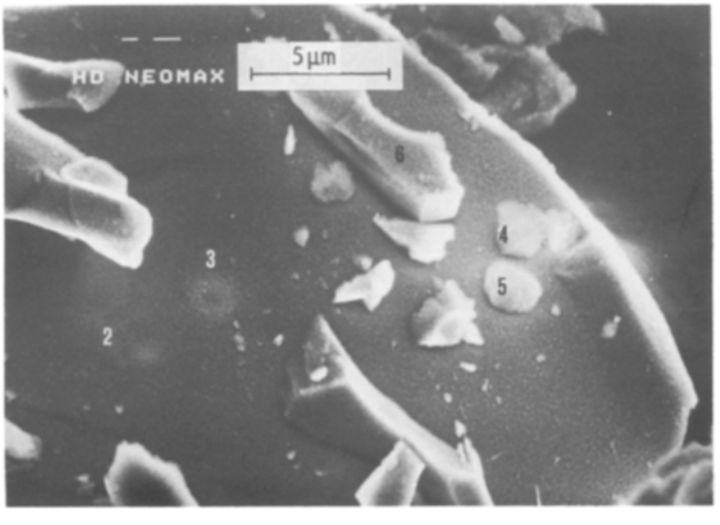

Figure 3 HD Neomax powder particle with fine debris on the surface.

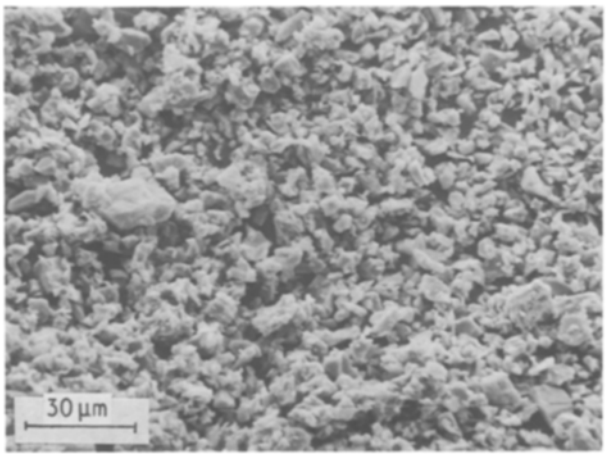

Figure 4 Typical HD/JM powder showing narrow distribution of particle size.

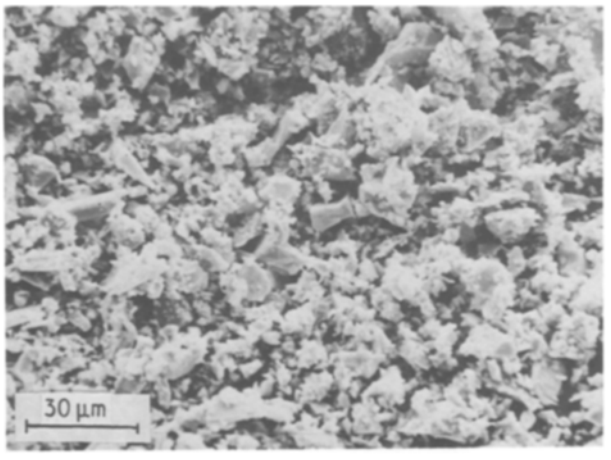

Figure 5 Typical HD/AM powder.

grain boundary. The description of the grain boundary phase as uniformly neodymium-rich is clearly an oversimplification, as the micrograph reveals it to be very complex.

2.2. Processing

In order to produce the fine powder necessary for the production of sintered magnets the following procedure was adopted.

(i) Bulk alloy castings were placed in a stainless steel hydrogenation vessel which was then evacuated to backing-pump pressure.

(ii) Hydrogen was then introduced into the vessel to a pressure of ~ 1 bar.

(iii) The hydrogen absorption process occurred after a short incubation period and was accompanied by audible clicks and a rise in temperature. The former is consistent with the decrepitation of the bulk material and the latter with the high exothermicity of the process [10, 12, 14].

(iv) The material produced during the hydrogen decrepitation process was transferred in 10 kg batches to the mill hopper. The milling process was carried out in a spiral-type jet mill, using a nitrogen atmosphere to produce the material suitable for pressing. Significantly shorter milling times were required than those needed to mill the conventionally pre-milled material.

(v) The hydrogen-decrepitated/jet-milled (HD/JM) powder was then pressed into an aligned green compact using a pressing force of between 1000 and 2500 $kg\,cm^{-2}$ and a perpendicular alignment field of 1000 $kA\,m^{-1}$.

(vi) The compacts were sintered over a range of temperatures from 960 to 1080° C, in a commercial vacuum furnace. A marked degradation in the vacuum at quite low temperatures ($\sim 200°$ C) was noted, due to the evolution of hydrogen from the $Nd_2Fe_{14}B$ matrix phase as the compacts were heated to the sintering temperature. This is in agreement with previous observations [8–11] on the hydrogen desorption behaviour of this material. The samples were maintained at the sintering temperature for 1 h and then slowly cooled to room temperature.

The sintered compacts were magnetized in a magnetic field of 2400 $kA\,m^{-1}$ prior to the determination of the second quadrant demagnetization loops.

3. Results and discussion

3.1. Characterization of the HD powder

The detailed morphology of the HD powder can be seen in Fig. 3. The powder consists of large pieces of

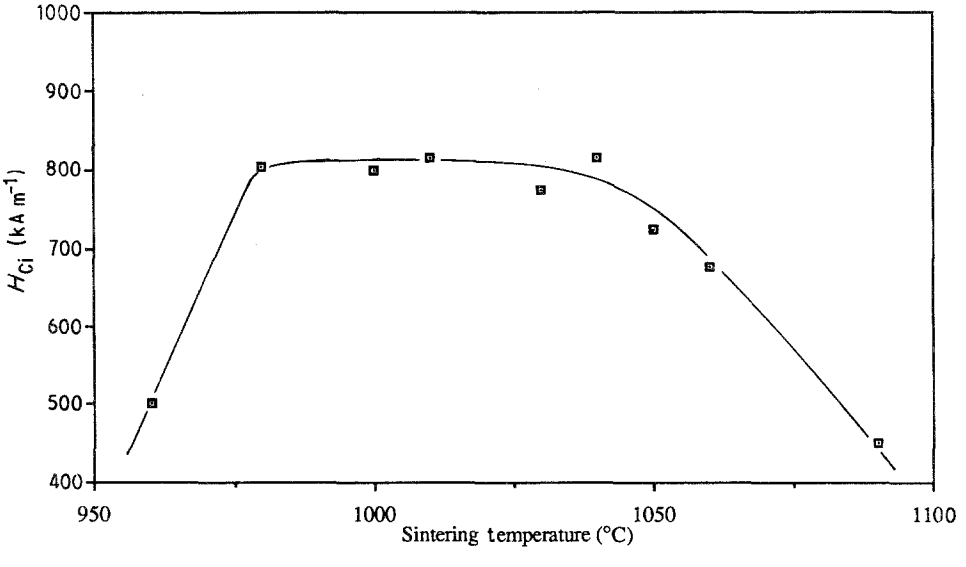

Figure 6 Variation of intrinsic coercivity with sintering temperature.

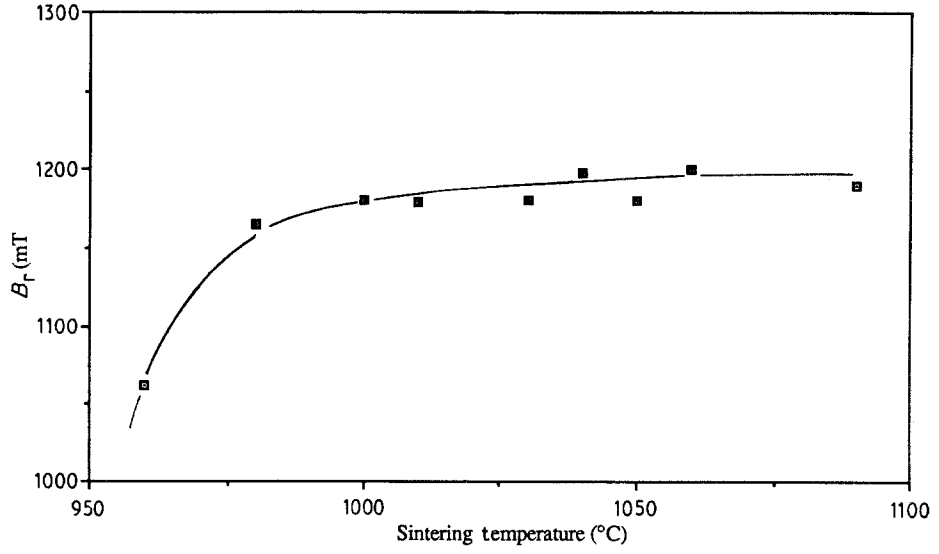

Figure 7 Variation of remanence with sintering temperature.

~ 50 to 100 μm with fine debris on the surface which is approximately 1 to 10 μm in size. Chemical analysis carried out on the material as a whole (⟨1⟩ in Table I) shows, as expected, that the Nd/Fe ratio was almost equal to 16/76. Slightly less neodymium-rich values were obtained from spot analysis on the large 50 to 100 μm pieces denoted by ⟨2⟩ and ⟨3⟩, indicating that their composition is somewhere between that of the $Nd_{16}Fe_{76}B_8$ starting alloy and the $Nd_2Fe_{14}B$ matrix phase.

The small disc-shaped debris, denoted by ⟨4⟩, ⟨5⟩ on the surface of the large pieces were found to have very high neodymium contens of up to a Nd/Fe ratio of 6.7/1, indicating that they are formed from the grain-boundary neodymium-rich phase. In addition a small number of pieces of ~ 10 μm denoted by ⟨6⟩ were found which had a Nd/Fe ratio indicating that they consisted primarily of the $NdFe_4B_4$-boride phase.

An oxygen analysis of the HD powder indicates a value of 0.15 wt %.

3.2. Characterization of the HD/JM powder

Typical HD/JM powder is shown in Fig. 4. For comparison, Fig. 5 shows typical powder produced by the HD/AM route. It is evident that the HD/JM powder exhibits an extremely uniform size, whereas a much wider range of particle size is obtained in the case of the HD/AM material. Fisher sub-sieve measurements on the HD/JM powder indicate a value of 2.3, comparable with that obtained for the HD/AM powder. An oxygen analysis of the HD/JM powder gives a value of 0.5 wt %.

3.3. Characterization of green compacts

The density of green compacts produced from HD/JM material was found to be significantly lower than similar compacts produced from standard attritor-milled and HD/AM material. It was found that to achieve a green compact density of 4 g cm^{-3} the HD/JM powder required a pressing force of 1500 kg cm^{-2} as opposed to the force of 1000 kg cm^{-2} needed for the HD/AM powder. This difficulty in achieving compact density has been attributed to the very narrow particle size distribution and the difficulty in packing such material.

Due to the effect hydrogen has on the magnetic anisotropy of the $Nd_2Fe_{14}B$ hard magnetic phase [15],

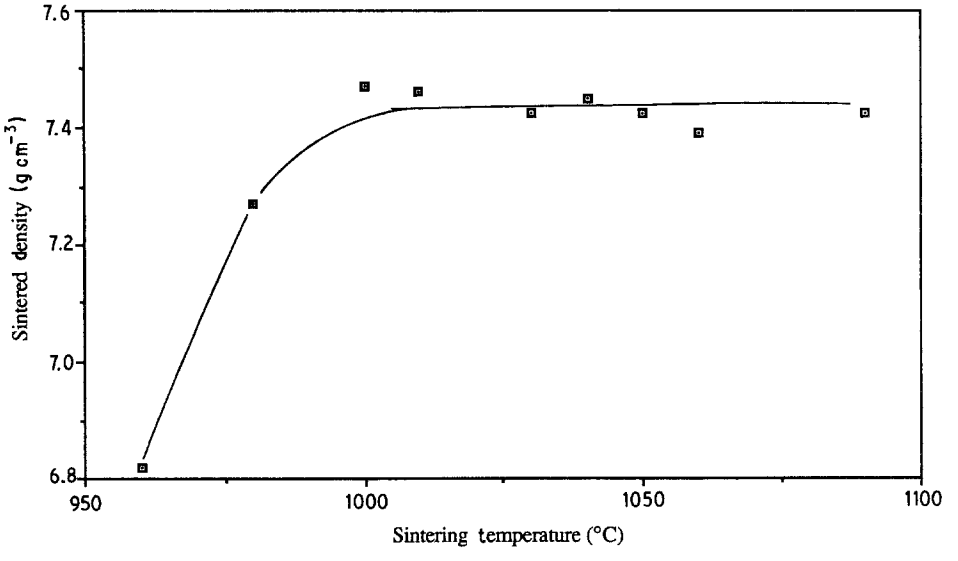

Figure 8 Variation of density with sintering temperature.

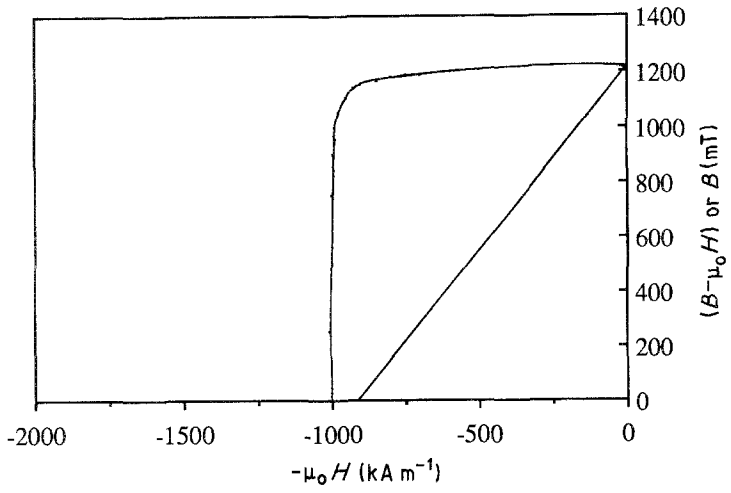

Figure 9 Demagnetization curve for $Nd_{16}Fe_{76}B_8$.

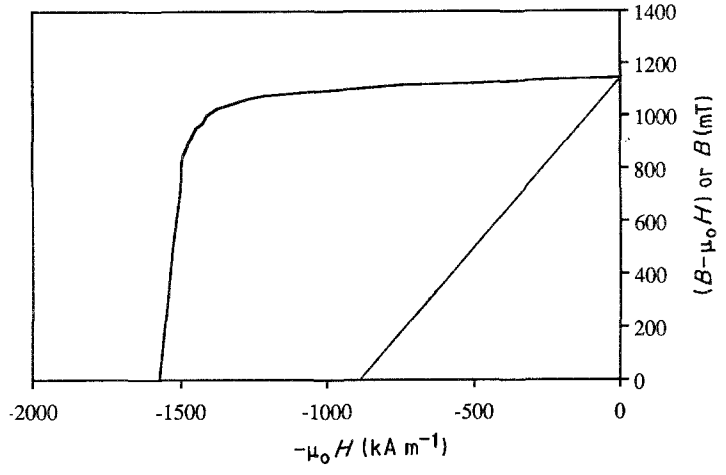

Figure 10 Demagnetization curve for $Nd_{14.5}Dy_{1.5}Fe_{76}B_7$.

the green compacts exhibited a much reduced coercivity in comparison with standard milled material. In previous studies [9] the alignment characteristics of HD/AM material were determined, and these studies established that hydrogen did not affect the uniaxial nature of the anisotropy so that HD/AM material could be fully aligned in a magnetic field. Similarly, no problems were encountered in achieving full alignment while processing the HD/JM material.

3.4. Characterization of sintered magnets

In order to establish the optimum sintering conditions, a study of the relationship between the properties of the HD/JM magnets and the sintering temperature has been carried out for the $Nd_{16}Fe_{76}B_8$ alloy and the results are shown in Figs 6, 7 and 8. The most striking feature of these graphs is the variation of H_{Ci} with sintering temperature. Little more than half the full intrinsic coercivity is realized by sintering at the usual sintering temperature of 1080° C and to achieve 800 kA m^{-1} the temperature must be reduced to below 1040° C for a 1 h sinter. The B_r-values of the material are not so dependent upon the sintering temperature except for compacts sintered below 1000° C, where the lack of a full sinter is reflected in the sharp drop in density from the fully dense value.

Typical $(B-\mu_0 H)$ against H curves for sintered and slowly cooled magnets made from HD/JM powder of the $Nd_{16}Fe_{76}B_8$ and $Nd_{14.5}Dy_{1.5}Fe_{76}B_7$ alloys are shown in Figs 9 and 10. The values of B_r, H_{CB}, H_{Ci} and BH_{max} are summarized in Table II together with typical values for magnets produced by the HD/AM process [9].

Metallographic examination indicates that the low coercivity observed in magnets sintered above 1040° C is due to excessive grain growth. Figs 11, 12 and 13 show qualitatively how the grain size increases with higher sintering temperatures.

A more quantitative examination was undertaken using a VIDS II Image Analyser system which combines the video output from a TV camera and microscope with the graphics display of an Apple computer

TABLE I Chemical analysis carried out on area of decrepitated material

Area	Nd/Fe ratio	Atomic ratio
Whole sample ⟨1⟩	0.228	17.3/76
Point ⟨2⟩ on large grain	0.198	15.1/76
Point ⟨3⟩ on large grain	0.195	14.8/76
Debris ⟨4⟩	6.69	6.69/1
Debris ⟨5⟩	2.70	2.70/1
Debris ⟨6⟩	0.256	1/3.9

TABLE II Magnetic parameters of magnets produced from hydrogen-decrepitated material

Property	$Nd_{16}Fe_{76}B_8$		$Nd_{14.5}Dy_{1.5}Fe_{76}B_7$
	HD/AM	HD/JM	HD/JM
B_r (mT)	1175 ± 5	1240 ± 5	1145 ± 5
H_{CB} (kA m^{-1})	690 ± 5	915 ± 5	875 ± 5
H_{Ci} (kA m^{-1})	740 ± 5	1010 ± 5	1570 ± 5
BH_{max} (kJ m^{-3})	250 ± 1	305 ± 1	260 ± 1

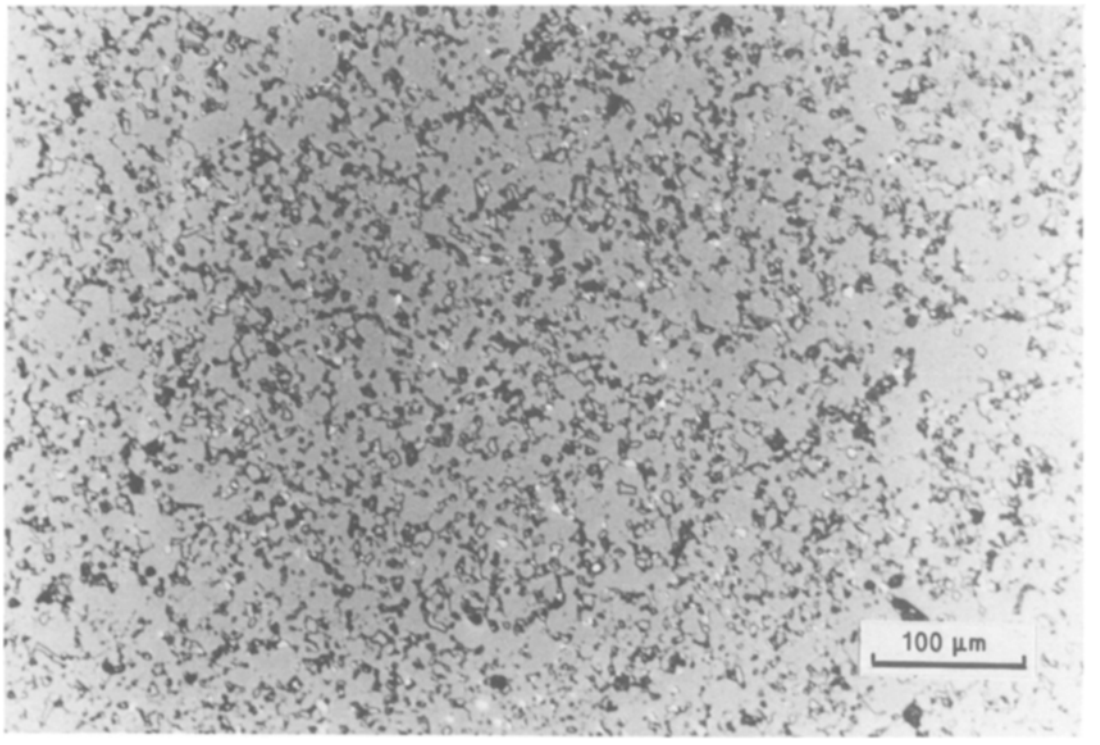

Figure 11 Micrograph of magnet sintered at 1010° C.

so that measurements may be made directly from the TV image. The VIDS II software is able to provide information on the grain size distribution as well as the mean grain size.

Fig. 14 shows how the grain size is affected by the sintering temperature. An increase in both average grain size and grain size distribution is observed, with material sintered at 1080° C having a mean size of greater than 20 μm. Measurements made on the coercivity of the sintered magnets (Fig. 6) indicate that an average grain size of $< 14\,\mu$m is necessary to achieve good coercivity from this particular alloy composition. Fig. 15, which shows how the spread of grain size varies with sintering temperature, indicates how important it is to maintain a narrow grain size distribution if good coercivities are to be obtained. The sharp increase in the range of grain sizes corresponds to the point where the coercivity begins to decrease.

The degree of grain growth at 1080° C, not normally observed in conventional processing, has been attributed to the clean, relatively debris-free material (Fig. 3) produced by the HD/JM process.

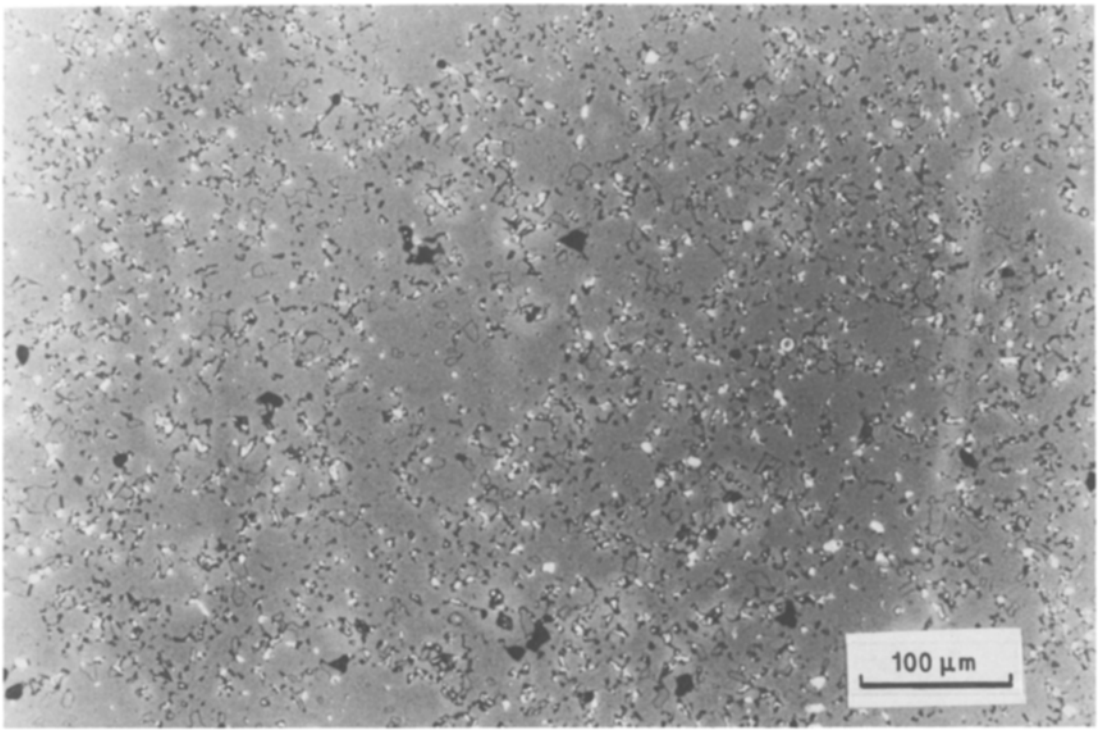

Figure 12 Micrograph of magnet sintered at 1050° C.

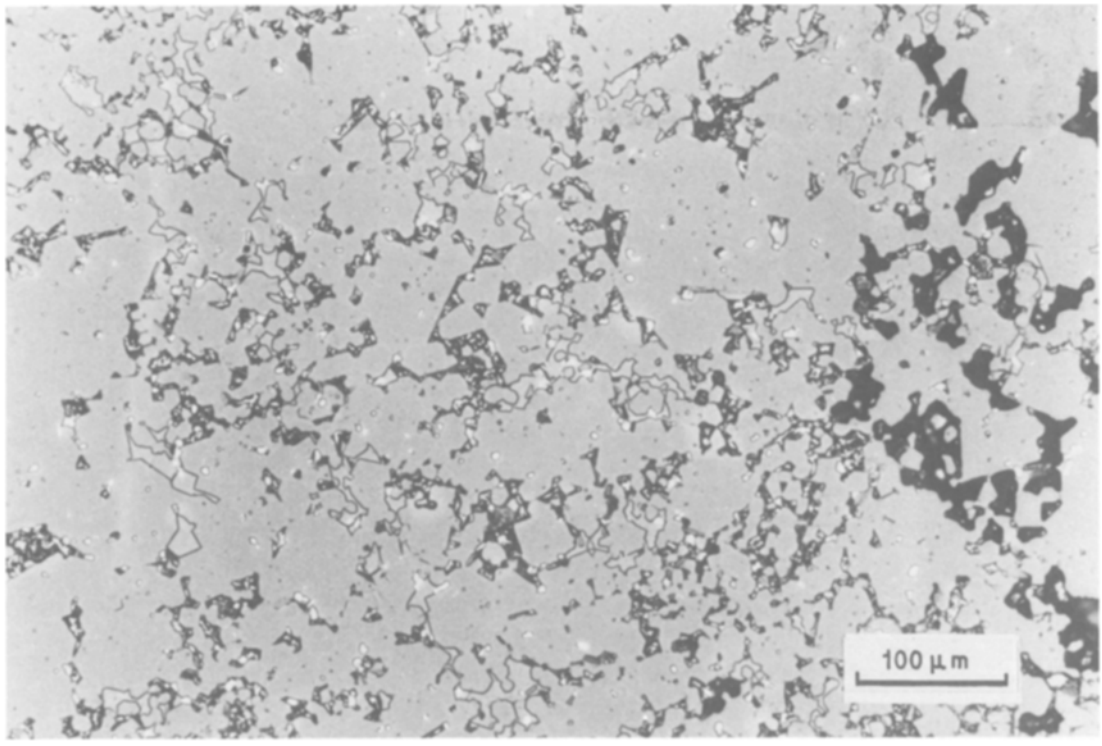

Figure 13 Micrograph of magnet sintered at 1080° C.

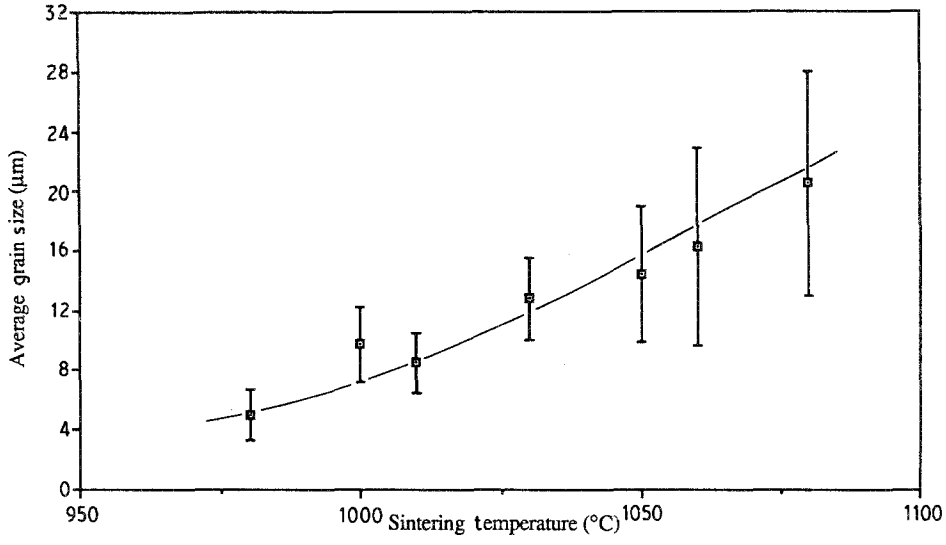

Figure 14 A graph showing the variation of grain size with sintering temperature.

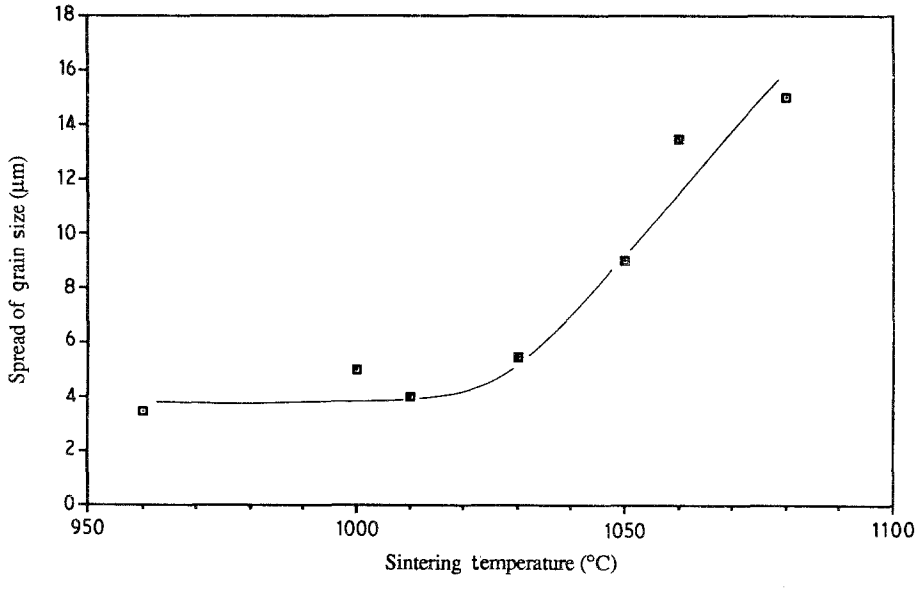

Figure 15 A graph showing how the spread of grain size varies with sintering temperature.

4. Conclusions

The combination of hydrogen decrepitation and jet milling has introduced several significant advantages over the conventional milling route in the production of permanent magnets.

1. Hydrogen decrepitation overcomes the problems of breaking up ingots, which can be extremely tough if they contain significant amounts of free iron.

2. Hydrogen decrepitation provides an inexpensive and straightforward method of producing large quantities of material suitable for either attritor or jet milling.

3. The extremely friable nature of the hydride enables it to be milled for a shorter time, in the case of attritor milling, or at a higher feed rate in the case of jet milling, when compared to conventionally pre-milled material.

4. The HD/JM material produced can be sintered at a temperature significantly below 1080° C and still achieve excellent properties.

References

1. I. R. HARRIS, *J. Less-Common Metals* **131** (1987) 245.
2. *Idem*, Paper No. 52 in Proceedings of 9th International Workshop on Rare Earth Magnets and their Applications, Bad Soden, August/September 1987, p. 267.
3. I. R. HARRIS, J. EVANS and P. S. NYHOLM, UK Patent 1 554 384 (1979).
4. A. KIANVASH and I. R. HARRIS, *J. Mater. Sci.* **19** (1984) 353.
5. *Idem, ibid.* **20** (1985) 682.
6. T. BAILEY and I. R. HARRIS, unpublished work.
7. M. SAGAWA, S. FUJIMURA, N. TOGAWA, H. YAMAMOTO and Y. MATSUURA, *J. Appl. Phys.* **55** (1984) 2083.
8. I. R. HARRIS, C. NOBLE and T. BAILEY, *J. Less-Common Metals* **106** (1985) L1.
9. P. J. McGUINESS, I. R. HARRIS, E. ROZENDAAL, J. ORMEROD and M. WARD, *J. Mater. Sci.* **21** (1986) 4107.
10. I. R. HARRIS, P. J. McGUINESS, D. G. R. JONES and J. S. ABELL, *Scripta Physica* **T19** (1987) 435.
11. J. M. CADOGAN and J. M. D. COEY, *Appl. Phys. Lett.* **48** (6) (1986) 442.
12. R. J. POLLARD and H. OESTERREICHER, *IEEE Trans. Magn.* **Mag 22** (1986) 735.
13. R. FRUCHART, R. MADAR, A. ROUAULT, P. L'HÉRITIER, P. TAUNIER, D. BOURSIER, D. FRUCHART and P. CHAUDOUET, French Patent No. 2556 758 (1986).
14. K. OESTERREICHER and H. OESTERREICHER, *Phys. Status Solidi (a)* **85** (1984) K1.

Received 7 April
and accepted 4 May 1988